

MITIGATION OF HIGH VOLTAGE BREAKDOWN OF THE BEAM SCREEN OF A CERN SPS INJECTION KICKER MAGNET

M.J. Barnes, W. Bartmann, M. Díaz, L. Ducimetière, L. Feliciano,
T. Kramer, V. Namora, D. Standen, T. Stadlbauer, P. Trubacova, F. Velotti, C. Zannini
CERN, Geneva, Switzerland

Abstract

The SPS injection kicker magnets (MKP) were developed in the 1970's, before beam induced power deposition was considered an issue. These magnets are very lossy from a beam impedance perspective: this is expected to be an issue during SPS operation with the higher intensity beams needed for HL-LHC. A design, with serigraphy applied to an alumina carrier, has been developed to significantly reduce the broadband beam coupling impedance and hence mitigate the heating issues. During high voltage pulse testing there were electrical discharges associated with the serigraphy. Detailed mathematical models have been developed to aid in understanding the transiently induced voltages and to reduce the magnitude and duration of electric field. In this paper, we discuss the solutions implemented to mitigate the electrical discharges while maintaining an adequately low beam-coupling impedance. In addition, the results of high voltage tests are reported.

INTRODUCTION

In CERN's Super Proton Synchrotron (SPS), a fast kicker system (MKP) is used for injection of the beam into the accelerator [1]. Two different types of the MKP magnets are used - the MKP-S and MKP-L. The MKP-S has an aperture of 100 mm wide by 61 mm high and the MKP-L aperture is 141.5 mm wide by 54 mm high: the width is the distance between the high voltage (HV) and return conductors. The two apertures are used to both meet optics requirements and provide the required deflection, within the constraints of available length and voltage and current demands on the pulse generators. The MKP magnets are transmission line type, constructed of multiple cells and operated in machine vacuum: the MKP-L has 22 cells.

As a result of the difference in the aperture dimensions, between the MKP-S and MKP-L modules, the real part of the beam coupling impedance of the MKP-L is generally significantly higher than that of the MKP-S [2]. Figure 1 shows temperature and pressure measurements, during March 2022, for an MKP-S and an MKP-L: the measured temperature rise of the MKP-L module is a factor of 3 to 4 times higher than for the MKP-S. The relatively large temperature rise of the MKP-L is attributable to its high beam coupling impedance. The temperature probes are mounted on the MKP side plate, which is at ground potential. Hence, the ferrite temperature will be higher than measured during beam induced heating [3]. The measured pressure in the MKP-L tank is considerably higher than for the MKP-S tank. The pressure consists of both a static component (without beam) and a

dynamic component (i.e. due to Electron cloud). The static pressure (the envelope of the base of the pressure) reaches a maximum of $\sim 5 \times 10^{-7}$ mbar for the MKP-L - this is mainly due to the heating of the ferrite: during the scrubbing, to avoid damage to the MKP-L modules, the measured temperature was purposefully limited to 70°C, and thus limited scrubbing [4]. The dynamic pressure, which is the difference between the envelope of the peak pressure and the static pressure, is also significant for the MKP-L.

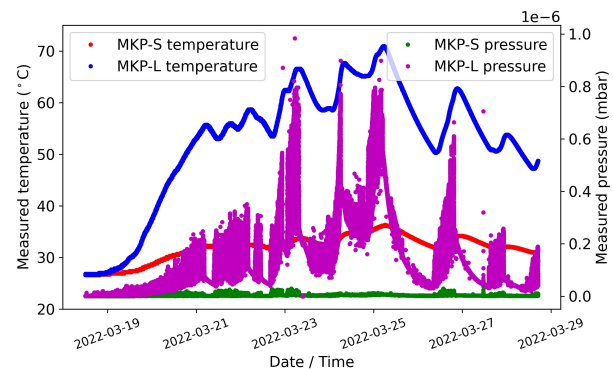


Figure 1: Temperature and pressure measurements, during March 2022, for an MKP-S module and an MKP-L module.

With the advent of higher bunch intensities for High Luminosity LHC, higher beam induced heating is expected in the ferrite yoke of the MKP-L, and will result in its Curie point being reached and unacceptably high static pressure. A design that mitigates the high heat load, which uses serigraphy, has been developed [2, 5, 6]. However, during high-voltage (HV) pulse testing, issues were encountered with the design: thus, it was necessary to re-optimize the design of the serigraphy for both beam impedance and HV behaviour.

SERIGRAPHY DESIGN

The cells of the MKP-L module are too short to apply serigraphy directly to the ferrite yoke [2]. Hence, a carrier is required to mechanically support the serigraphy in the aperture: alumina has been chosen for this purpose. The alumina will reduce the aperture available to the beam in the MKP-L's. Hence, a detailed model of the injection region has been constructed and subsequent aperture studies carried out [7]. These studies defined both the required beam aperture and good field regions at the entrance and exit of the MKP-L magnet [7], and hence defined the maximum thickness of the alumina.

During HV pulse conditioning a Pulse Forming Network (PFN), which is charged to a positive voltage, is discharged

into a matched impedance MKP-L module which is terminated with a matching resistor (TMR). A Penning gauge is mounted on the MKP-L vacuum tank. The tank has a clear window to allow observation of the MKP-L aperture from one end. In general, the pulse repetition rate during conditioning was 10 s. The 10 s allows a pressure rise which is not due to a breakdown to recover between pulses. During the conditioning, the PFN voltage is ramped slowly from 12 kV up to 54 kV, with a pulse length of 1 μ s: the nominal number of pulses, during the ramp, is \sim 32,000. During operation in the SPS, the nominal PFN voltage is 49 kV: the 54 kV PFN gives \sim 10% margin. If the vacuum rises above pre-defined thresholds, during the conditioning, the PFN voltage is automatically reduced and then slowly ramped up again. Once the ramping is complete, the PFN voltage is reduced to 53 kV and the pulse length extended to 3 μ s.

Serigraphy Referenced to Ground Potential

The original (V1) serigraphy consisted of five silver fingers, each 600 mm long, on each of two alumina plates, three fingers from one end of the plate and two from the other [2,5]: the two sets of fingers were capacitively coupled together, via the permittivity of the alumina plates. The serigraphy was connected to the end ground plates of each MKP-L which, in the SPS, would be connected to the beam pipe. Both CST [8] predictions and measurements confirmed that the real beam coupling impedance of this MKP-L was adequately low [6].

In V1 the alumina plates were supported, on each side, by grooves cut into both the HV and return busbars. During HV pulse conditioning corona was observed between the serigraphy finger closest to the HV busbar and the HV busbar at a PFN voltage of only 35 kV: a pressure rise of 3×10^{-8} mbar was observed at each pulse.

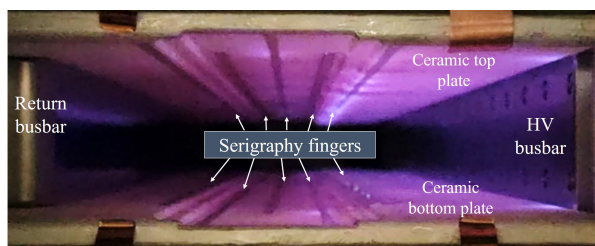


Figure 2: MKP-L V2: corona during HV pulsing, with serigraphy connected to end ground plates, 50 kV PFN.

In the second design iteration (V2) the alumina plates were moved to give a 5 mm gap between the HV busbar and the alumina plates. Although the MKP-L was conditioned to 54 kV PFN, there was a pressure rise of 1×10^{-8} mbar during each pulse at 50 kV PFN: there was significant corona associated with the serigraphy (Fig. 2). The pressure rise increased with pulse length. Simulations showed that, during the flat-top, when the HV busbar and ferrite are at a potential of half the initial PFN voltage and the serigraphy is at ground potential, there is a very high electric field associated with the sharp edges of the serigraphy. To mitigate the electric field during the pulse flat-top the design was modified so

that the serigraphy was referenced to the HV end plates (V3), which sandwich the complete ferrite yoke.

Serigraphy Referenced to HV End Plates Potential

Referencing the serigraphy to the HV end plate ensures that the serigraphy still covers the ferrite yoke (Fig. 3): however, a 10 mm gap between the HV and ground end plates is no longer covered by the serigraphy. Beam impedance simulations and measurements showed that the gap did not introduce a geometrical impedance resonance and the predicted beam induced power deposition was even further decreased in comparison with connecting the serigraphy to the end ground plates.

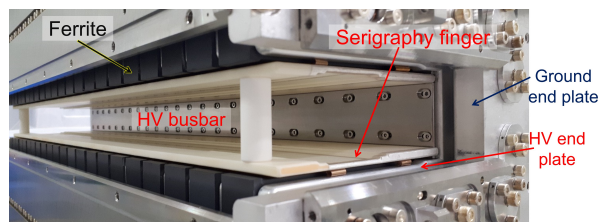


Figure 3: MKP-L V3, with serigraphy connected to HV end plates. For clarity, no return busbar is mounted (it would close the left hand side of the aperture).

Figure 4 shows corona during HV pulsing, which occurs close to the end of serigraphy fingers #3 and #5: these fingers are connected to the HV end plate at the TMR end of the MKP-L module. No corona was observed at the TMR end of the module during this test. The pressure rise measured was $\sim 2 \times 10^{-9}$ mbar per pulse – which recovered before the next pulse. The module was also pulsed from the opposite end: the corona always occurred at the pulse input end of the module. Nevertheless, the reduction in corona, of V3 versus V2, is clearly visible by comparing Figs. 2 and 4.

The corona in Fig. 4, is visible above \sim 25 kV PFN voltage. The pulse takes \sim 200 ns to propagate through the module (fill time). During the fill time the serigraphy referenced to the output HV end plate (fingers #1, #3 and #5) are at a lower potential than fingers #2 and #4, which are referenced to the input HV end plate. However, there is voltage induced on each serigraphy, during field rise and fall times, whose magnitude depends upon the position of the serigraphy with respect to the return busbar: #5 has the lowest induced voltage while #1 has the highest. Fingers #3 and #5 are the most susceptible to corona as they have the largest potential difference with respect to the ferrite yoke during the fill time.

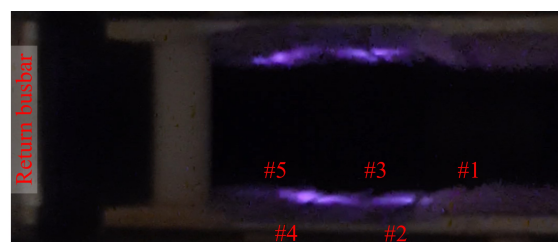


Figure 4: MKP-L V3, with serigraphy connected to HV end plates: corona at end of serigraphy #3 and #5: 51 kV PFN.

A detailed PSpice equivalent circuit, with self and mutual inductances and also capacitance for the serigraphy in each cell of the MKP-L module, was derived from Opera2D [9] simulations. PSpice was used to study the influence of various parameters, including the length of the serigraphy and its horizontal position in the aperture. In addition, CST simulations were carried out to study the influence of the length of the serigraphy upon beam impedance and beam induced power deposition. Based on these predictions it was proposed to eliminate serigraphy finger #5 and to decrease the length of all serigraphy fingers, in particular #1 and #3.

CST predictions, subsequently verified by measurements, confirmed that finger #5 could be eliminated. In addition, the length of serigraphy fingers #1 and #3 were reduced from 600 mm to 457 mm and #2 and #4 were reduced from 600 mm to 581 mm. The first significant resonance in the real beam coupling impedance was at a frequency of ~30 MHz: this is considered sufficiently far from the first beam harmonic (40 MHz), with 25 ns bunch spacing, and also from 20 MHz if 50 ns bunch spacing were to be considered again in the future. Furthermore, simulations showed that the electric field, which is highest at the end of finger #3, could be further reduced by including either a 'groove' or a 'slot' in the alumina (see Fig. 5): this was the V4 serigraphy.

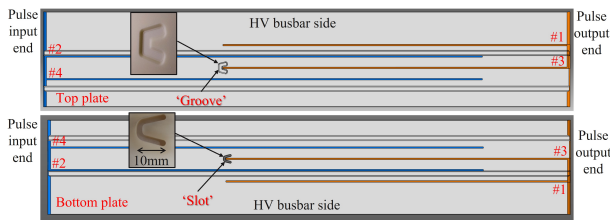


Figure 5: MKP-L V4, with four serigraphy fingers per plate, connected to HV end plates: #1 and #3 of 457 mm length.

With the V4 serigraphy corona was still observed, but at a much reduced intensity compared to V3. In addition, the corona, which was mainly on the end of finger #3, was not observed below 35 kV PFN. The measured pressure rise, was approximately 2×10^{-9} mbar per pulse - which recovered before the next pulse. Again there was no corona observed at the TMR end. A comparison of the intensity of light associated with the top and bottom plates indicated that the groove was slightly better (lower intensity) than the slot.

The V4 module was pulsed for a total of ~180,000 pulses, the majority of which were at 52 kV PFN and 2 μ s pulse length. Subsequently, the beam coupling impedance of the module was remeasured, and the serigraphy carefully inspected. The impedances before and after HV pulse conditioning were in good agreement with each other - hence no degradation of serigraphy was apparent. In addition, microscope inspection of the finger #3, next to the slot, showed no damage. However, in order to further reduce the electric field at the end of serigraphy #3, impedance simulations were carried out to determine the minimum acceptable length.

The CST simulations indicated that it was acceptable to reduce the length of serigraphy #1 and #3 by a further 93 mm

to 364 mm. PSpice simulations showed that this should reduce the duration of the voltage stress on finger #3 by ~17%: hence this was the baseline for the V5 serigraphy, together with the groove at the end of finger #3. In addition, because the existing MKP-L modules suffer from electron cloud, and thus dynamic pressure issues (Fig. 1), it is preferable to utilize a closed alumina chamber (Fig. 6). It is planned to magnetron sputter the beam aperture side of the alumina with Cr_2O_3 , to reduce its secondary electron yield (SEY) [10]. However, if electron cloud occurs the closed chamber prevents a conducting path between the serigraphy (which is at HV during injection of beam) and the return conductor.

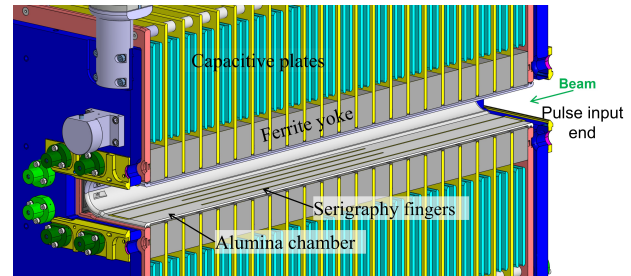


Figure 6: Cross-section of a 3D model of the MKP-L.

During HV pulsing of V5, the return busbar side of the alumina chamber, at the pulse input end, showed light. The intensity was dependent upon both pulse voltage and duration, and caused a pressure rise on each pulse, of $\sim 1.7 \times 10^{-8}$ mbar at 43 kV PFN and 1 μ s pulse width. When the module was pulsed from the other end, with the same polarity of voltage, the light moved to the HV busbar side of the chamber: this suggests a source of electrons being steered by the magnetic field. The light is thought to be produced by electrons impacting the alumina causing desorption of gas [11]: the SEY of the alumina (likely to be ~1.5 at 20 keV [12]) ionises the desorbed gas. Subsequently, the alumina chamber was coated with aC, to reduce its SEY, and a 5 mm conductor was used to close the C-shaped aperture of the HV end plate at the pulse input end. This MKP-L was successfully HV pulse conditioned: the pressure rise was $\sim 5 \times 10^{-10}$ mbar at 50 kV PFN, and continued to decrease with conditioning. The pressure rise was independent of pulse length.

CONCLUSION

Serigraphy, for reducing beam induced heating, is connected to the HV end plates of the MKP-L to reduce the electric stress during pulsing. The number of serigraphy fingers and their length has been optimised for both HV and beam impedance considerations: in the final design a total of eight serigraphy fingers are used with the shortest fingers connected to the HV end plate at the pulse output end.

ACKNOWLEDGEMENTS

The authors acknowledge the contributions of many colleagues for their preparation of the MKP-L module, including: G. Bellotto, P. Burkel, D. Comte, P. Goll, F. Pelloux, Y. Sillanoli, M. van Stenis, M. Taborelli and W. Vollenburg.

REFERENCES

- [1] P.E. Faucher *et al.*, “The SPS fast pulsed magnet systems”, in *Proc. 12th IEEE Modulator Symposium*, New York, NY, USA, Feb. 1976, pp. 1-27.
- [2] M. Beck, “Simulation, measurement and mitigation of the beam induced power loss in the SPS injection kickers, Master: KIT, Karlsruhe: 2015-09-23, CERN-THESIS-2015-374.
- [3] F. M. Velotti, M. J. Barnes, B. Goddard, and I. Revuelta, “Fortune Telling or Physics Prediction? Deep Learning for On-Line Kicker Temperature Forecasting”, presented at the 13th Int. Particle Accelerator Conf. (IPAC’22), Bangkok, Thailand, Jun. 2022, paper TUPOST044, this conference.
- [4] V. Kain *et al.*, “Achievements and Performance Prospects of the Upgraded LHC Injectors”, presented at the 13th Int. Particle Accelerator Conf. (IPAC’22), Bangkok, Thailand, Jun. 2022, paper WEIYGD1, this conference.
- [5] M. J. Barnes *et al.*, “Studies of Impedance-related Improvements of the SPS Injection Kicker System”, in *Proc. 7th Int. Particle Accelerator Conf. (IPAC’16)*, Busan, Korea, May 2016, pp. 3611–3614. doi:10.18429/JACoW-IPAC2016-THPMW030
- [6] M. J. Barnes, O. Bjorkqvist, and K. Kodama, “Beam Induced Power Deposition in CERN SPS Injection Kickers”, in *Proc. 12th Int. Particle Accelerator Conf. (IPAC’21)*, Campinas, Brazil, May 2021, pp. 3490–3493. doi:10.18429/JACoW-IPAC2021-WEPAB342
- [7] A. Mahon, M.A. Fraser, F. Velotti, “Construction of TT10-SPS Injection Region Model and Following Aperture Studies”, CERN-ACC-NOTE-2018-0074.
- [8] Dassault Systèmes, CST Studio Suite, <https://www.3ds.com/products-services/simulia/products/cst-studio-suite/>.
- [9] Cobham, Opera-2d User Guide v18R2, https://www.cobham.com/media/637229/cts_vectorfields_opera_240610.pdf
- [10] M.J. Barnes, C. Bracco, G. Bregliozzi, A. Chmielinska, L. Ducimetière, B. Goddard, *et al.*, “Operational Experience of a Prototype LHC Injection Kicker Magnet with a Low SEY Coating and Redistributed Power Deposition”, in *Proc. IPAC’19*, Melbourne, Australia, May 2019, pp. 3974–3977, doi:10.18429/JACoW-IPAC2019-THPRB072
- [11] H. C. Miller, “Flashover of insulators in vacuum: the last twenty years,” in *IEEE Transactions on Dielectrics and Electrical Insulation*, vol. 22, no. 6, December 2015, pp. 3641-3657. doi:10.1109/TDEI.2015.004702
- [12] Y. Kijima, Co. Ltd, S. Mitsunobu, T. Furuya, and R. Noer, “The Secondary Electron Yield of the Material for the KEKB Superconducting Cavity Input Coupler”, in *Proc. 10th Workshop RF Superconductivity (SRF’01)*, Tsukuba, Ibaraki, Japan, Sep. 2001, pp. 560-564, paper PT027.